

Accelerating Multimodal Large Language Models via Dynamic Visual-Token Exit and the Empirical Findings

Qiong Wu¹, Wenhao Lin¹, Weihao Ye¹, Yiyi Zhou¹, Xiaoshuai Sun¹, Rongrong Ji¹

¹ Key Laboratory of Multimedia Trusted Perception and Efficient Computing, Ministry of Education of China, Xiamen University, 361005, P.R. China.

{qiong, wenhaolin, weihaoye}@stu.xmu.edu.cn, {zhouyiyi, xssun, rrji}@xmu.edu.cn

Abstract

The excessive use of visual tokens in existing Multimodal Large Language Models (MLLMs) often exhibits obvious redundancy and brings in prohibitively expensive computation. To gain insights into this problem, we first conduct extensive empirical studies on the attention behaviors of MLLMs, and summarize three main inference stages in MLLMs: (i) Early fusion between tokens is first accomplished quickly. (ii) Intra-modality modeling then comes to play. (iii) Multimodal reasoning resumes and lasts until the end of inference. In particular, we reveal that visual tokens will stop contributing to reasoning when the text tokens receive enough image information, yielding obvious visual redundancy. Based on these generalized observations, we propose a simple yet effective method to improve the efficiency of MLLMs, termed dynamic visual-token exit (DyVTE). DyVTE uses lightweight hyper-networks to perceive the text token status and decide the removal of all visual tokens after a certain layer, thereby addressing the observed visual redundancy. To validate VTE, we apply it to a set of MLLMs, including LLaVA, VILA, Eagle and InternVL, and conduct extensive experiments on a bunch of benchmarks. The experiment results not only show the effectiveness of our VTE in improving MLLMs' efficiency, but also yield the general modeling patterns of MLLMs, well facilitating the in-depth understanding of MLLMs. Our code is anonymously released at <https://github.com/DoubtedSteam/DyVTE>.

1. Introduction

Recently, the rapid development of vision-language learning has been witnessed with the great success of large language models (LLMs) [1, 2, 6, 19, 28, 49, 50, 57]. Numerous efforts are devoted to equipping LLMs with general multimodal capability, i.e., multimodal large language models (MLLMs) [3, 12, 33, 40, 53]. To overcome vi-

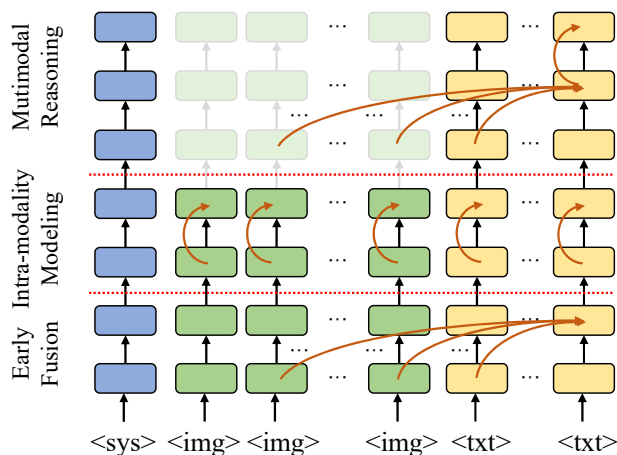


Figure 1. Illustration of three main stages observed in MLLMs. During inference, an MLLM will gradually go through three main stages, i.e., early fusion between all tokens, intra modality modeling of the same-modal tokens, and multimodal reasoning between all tokens again. When the text tokens receive enough image information, visual tokens will stop contributing to inference regardless of their activities. Based on this observation, we propose a novel dynamic visual-token exit (DyVTE) method for MLLMs.

sual shortcoming [46, 60], recent MLLMs often resort to higher-resolution images as input, which is often accompanied with a multitude of visual tokens [12, 33, 45, 53].

Despite effective, the excessive use of visual tokens also leads to prohibitively expensive computation. For instance, compared with LLaVA 1.5 [40], LLaVA-NeXT [33] adopts about 1728 more visual tokens, resulting in about 4 times FLOPs. Moreover, recent progresses also show that these visual tokens often exist heavy redundancy in MLLMs. For instance, Ye *et al.* [59] show that randomly dropping half visual tokens barely affects the performance on common VL tasks, such as MMB [41] and SQA [42]. In this case, the efficient use of visual tokens has recently become a research hot-spot, attracting an influx of attention [7, 9, 16, 52, 54].

To gain insights into visual redundancy in MLLMs, we first conduct extensive empirical studies about the attention behaviors of MLLMs, and summarize three main stages of their inference, as illustrated in Fig.1. At the first stage, an MLLM quickly accomplishes the exchange of multimodal information at its shallow layers, which we term *(i) early fusion*. Afterwards, this information exchange fades away, and the self-attention between tokens of the same modality becomes the main activity in the second stage, termed *(ii) intra-modality modeling*. At the last stage, the visual tokens will resume the information propagation to the text tokens, and this process will continue until the end of inference, and we term it *(iii) multimodal reasoning*. Through extensive comparisons, we reveal that these observed behaviors of MLLMs are generalized across different models [11, 37, 40, 45] and tasks [26, 27, 41, 46, 60], as shown in our experimental section.

Behind these general behaviors of MLLMs, we also observe interesting findings directly related to visual redundancy. As summarized above, the visual tokens will continue to diffuse their semantics to the text ones at the multimodal reasoning stage, while its self-modeling also often plays at the same time. However, we find that this cross-modal interaction in fact barely contributes to multimodal reasoning after some layers. In other words, multimodal reasoning basically acts within text tokens when the text tokens receive enough visual semantics. For instance, dropping all visual tokens at some top layers of MLLMs barely impedes the prediction and also makes not obvious changes to the self-attention patterns of text tokens, as shown in our experimental section. Overall, these results imply that visual tokens can in fact exit at a certain layer of MLLMs without affecting the following reasoning.

Motivated by these observations, we propose a simple yet effective method for improving MLLMs’ efficiency in this paper, termed *dynamic visual-token exit* (DyVTE) as depicted in Fig.2. In particular, we apply lightweight hyper-networks to perceive text token status and decide the removal of all visual tokens, thereby improving efficiency and speeding up inference. Compared with previous efforts like *visual token pruning* [4, 8], we study the efficiency issue of MLLMs from a new perspective, *i.e.*, perceiving the learning status of text tokens about multimodal reasoning rather than evaluating the redundancy of specific visual tokens. Moreover, these two strategies are orthogonal and can work collaboratively, as proven in our experiments. In addition, DyVTE also greatly differs from common *dynamic early exiting* methods [10, 21, 25, 48], which often refers to a inference break, *i.e.*, skipping the rest layers for a direct prediction. In contrast, text tokens will continue to transform in DyVTE, which better meets our empirical findings.

To validate DyVTE, we apply it to a set of advanced MLLMs with varying scales, including LLaVA-1.5 [40],

VILA [37], Eagle [45] and InternVL [11], on a bunch of widely-used VL and MLLM benchmarks [24, 26, 27, 35, 46, 60]. The experimental results show that our DyVTE can greatly reduce the computation overhead of MLLMs, while still maintaining their competitive performance on various benchmarks. For instance, our DyVTE reduces the computation overhead of LLaVA-1.5 by up to 45.7% without significant performance drops. Moreover, DyVTE is fully compatible with the widely used *Flash Attention* [13] and some visual token pruning methods like FastV[8].

Overall, our contributions are three-fold:

- We observe and summarize three main stages of MLLMs during inference, and reveal the dependency between text token status and visual redundancy, which are generalized across models and tasks.
- Based on these empirical findings, we propose a simple yet effective method to address the visual redundancy of MLLMs, termed *dynamic visual-token exit* (DyVTE).
- The extensive experiments on a set of MLLMs well validate the motivation and effectiveness of DyVTE, facilitating the future research of MLLMs.

2. Related Work

Driven by the success of *large language models* (LLMs) [1, 2, 17, 19, 28], the decoder-only paradigm model is also used as the main modeling approach of *multimodal large language models* (MLLMs) [3, 12, 33, 34, 40]. In MLLM, visual information is added mainly by using visual tokens as an extension of the input sequence. For instance, BLIP-2 [34] introduces QFormer which alleviates the modality gap while taking the most relevant content of the text as the extension of the input sequence. Qwen-VL [3] uses learnable tokens and cross-attention to collect information from image features and expand the input sequence. LLaVA [40] uses a projection layer to map visual features into the semantic space of the LLM, and take all visual tokens to expand the input sequence. Recently, in order to achieve better performance, MLLMs have invariably increased the resolution of the input image. It significantly increases the length of the input sequence. For example, LLaVA-OneVision [33] improves the resolution of the input image by dividing the high-resolution image into several regions and extracting features separately. InternVL-1.5 [12] not only introduces a stronger visual encoder, but also sets different input resolutions and scales the input image to the closest aspect ratio as the input of the visual encoder. Similarly, Qwen2-VL [53] shares the dynamic resolution with InternVL-1.5, and also proposes a carefully designed Position Embedding for various input formats. In summary, increasing resolution brings significant performance improvements, but also a significant increase in computational overhead.

To maintain the powerful capabilities of MLLMs while

enhancing their efficiency, several recent works have focused on improving the computational efficiency of MLLMs. These methods, primarily in transformer-based networks [15, 18, 51], can be categorized into three main approaches: model architecture [23, 36, 55, 56, 61], dynamic reasoning [14, 20, 21, 38, 47], and token pruning [29, 43, 44, 58]. Works in model architecture [36, 55, 56] improve the efficiency of MLLMs by sparsifying the model structure. For instance, MoE-LLaVA [36] selectively activates the most relevant feedforward networks (FFNs) from a set of parallel FFNs, treating the selected FFN as the expert for the input. Similarly, RoE [55] models an MLLM as a mixture-of-experts (MoE) model, where only a subset of layers is activated, constructing a more effective and efficient expert model for each input. In the dynamic reasoning approach [10, 21], efficiency gains are achieved by terminating inference early, *i.e.*, skipping the remaining layers. AdaInfer [21], for example, predicts the confidence of decoding tokens and terminates inference when sufficient confidence is reached. Beyond top-1 [38] analyzes the decoding token determination rules in LLMs, halting reasoning once the second-most confident token appears, thus reducing unnecessary computation. Token pruning methods [5, 16, 22, 30, 52, 54] improve reasoning efficiency by removing task-irrelevant visual tokens. FastV [8] prunes tokens based on the average attention each token receives, eliminating those deemed less important. FitPrune [59] maintains the original attention distribution during pruning, ensuring the MLLMs’ attention mechanisms remain intact. In contrast to these approaches, we propose a simple yet effective method called *dynamic visual-token exit* (DyVTE). By observing the pattern of MLLMs, DyVTE removes visual tokens when they no longer contribute meaningfully to multimodal reasoning, optimizing efficiency while maintaining model performance.

3. Dynamic Visual-token Exiting

3.1. Method

In this paper, we propose a simple yet effective method to reduce the visual redundancy of MLLMs, termed *dynamic visual-token exit* (DyVTE). As discussed above, DyVTE uses lightweight hyper-networks to perceive the text token statuses of MLLMs, thereby judging the right time to remove all visual tokens to improve efficiency.

As shown in Fig.2, given the text tokens $\mathbf{T}^{(k)}$ at the k -th layer of an MLLM, we use a simple MLP as the hyper-network to learn their statuses and decide whether to remove all visual tokens, defined by

$$\mathbf{p} = \text{Softmax}(\text{GELU}([\text{avg}(\mathbf{T}_{1:t-1}^{(k)}), \mathbf{T}_t^{(k)}] \mathbf{W}_1) \mathbf{W}_2), \quad (1)$$

where $\mathbf{p} \in \mathcal{R}^2$ is the binary prediction, $\mathbf{W}_1 \in \mathcal{R}^{2d \times h}$ and $\mathbf{W}_2 \in \mathcal{R}^{h \times 2}$ are weight matrices, and h is the dimension

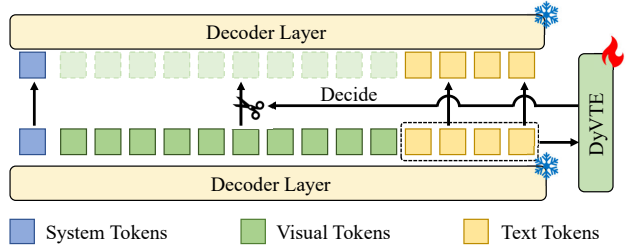


Figure 2. Illustration of the proposed *dynamic visual-token exit* (DyVTE). Our DyVTE aims to early exit visual tokens according to the prediction of a lightweight hyper-network based on text token status, thus achieving better efficiency for MLLMs.

of the hidden states. Here, the hyper-network uses two token representations, *i.e.*, $\text{avg}(\mathbf{T}_{1:t-1})$ and \mathbf{T}_t . The former represents the average state of most text tokens. Besides, we also use the last text token $\mathbf{T}_t^{(k)}$ as reference, since it often plays an important role in decoding under the *unidirectional self-attention* operation of MLLMs [39, 47].

When the prediction \mathbf{p} refers to early visual-token exit at l -th layer, DyVTE will remove all visual tokens at this layer, while keeping the text tokens continues to transform in MLLMs. Given an input sample $[\mathbf{V}, \mathbf{T}]$, DyVTE first gain the text tokens $\mathbf{T}^{(l)}$ and visual tokens $\mathbf{V}^{(l)}$ at l -th layer:

$$[\mathbf{V}^{(l)}, \mathbf{T}^{(l)}] = G_{1:l}([\mathbf{V}, \mathbf{T}]), \quad (2)$$

where $G_{1:l}(\cdot)$ represents the transformation of the first l layers in the MLLM. Then all visual tokens are removed, and the final output P'_l with DyVTE is obtained by

$$P'_l = G_{l+1:L}(\mathbf{T}^{(l)}), \quad (3)$$

where $G_{l+1:L}(\cdot)$ denote the remaining layers in the MLLM.

In particular, given sufficient early-exit examples, DyVTE can learn to judge the text token statuses at each layer of the MLLM. Thus, its accurate removals of visual tokens will greatly speed up the inference in the rest layers of the MLLM, while retaining similar predictions.

3.2. Optimization

The target of DyVTE is to correctly predict the exit layer of visual tokens without affecting its final outputs. In this case, its objective can be defined by

$$\underset{\theta_h}{\text{argmin}} d(P, P'_l), \quad (4)$$

where θ_h denotes the weights of hyper-networks in DyVTE. $d(\cdot, \cdot)$ is an distance functions [31]. And P'_l and P are the predictions of an MLLM with and without early visual token exit, respectively.

To directly optimize Eq.4, a viable way is to merge predictions of hyper-networks with visual tokens of MLLMs,

e.g., attention masks based on *Gumbel softmax*, thus using the *next token prediction* loss to indirectly update DyVTE. Although the MLLM can be fixed, but the complete computation of the whole model’s gradients are still required, which is often inefficient and expensive.

Considering the target of DyVTE is to find out the optimal step for visual-token exit, we can actually train the hyper-networks independent to the gradient back-propagation of MLLMs, *i.e.*, directly proper supervision.

Concretely, we can compare the discrete outputs of the MLLM with and without DyVTE, *e.g.*, the answer strings A . If the answers are exactly the same, we can give a positive feedback to hyper-networks, and *vice versa*. By comparing it with the default output A , we can judge that whether the current input should be exited at i -th layer:

$$\mathbf{y} = \begin{cases} 1, & A'_i = A, \\ 0, & A'_i \neq A. \end{cases} \quad (5)$$

Here, A'_i denotes the answer predicted with visual-token exit at the i -th layer. Besides, to make this supervision more robust, we also consider the prediction uncertainty, making the model behaviors akin more to the case without exit:

$$\mathbf{y} = \begin{cases} 1, & A'_i = A \wedge \rho'_c < \tau, \\ 0, & \text{otherwise.} \end{cases} \quad (6)$$

Here, ρ'_c denotes the prediction uncertainty, represented by *cross-entropy*, and τ denotes the threshold, which is the default uncertainty ρ_c multiplied by a scale value.

With this supervision, the hyper-networks in DyVTE can be optimized by the cross-entropy loss:

$$\mathcal{L}_D = -(\mathbf{y} \cdot \log(\mathbf{p}_1) + (1 - \mathbf{y}) \cdot \log(\mathbf{p}_0)). \quad (7)$$

In practice, we randomly sample exit layers at each training step, and give the weak labels according to Eq.6, based on which the hyper-networks are optimized by Eq.7.

4. Experiment

4.1. Datasets and Metrics

The benchmarks used in this paper consist of four conventional vision-language (VL) benchmarks and five newly introduced MLLM benchmarks. The traditional VL benchmarks include VQAv2 [26], GQA [27], ScienceQA [42], and TextVQA [46]. The MLLM benchmarks comprise POPE [35], MME [24], MMB [41], SEED [32] and MM-Vet [60]. Unlike general VL evaluations, these benchmarks are designed to assess MLLMs from diverse views, such as *fine-grained reasoning* [60] and *visual hallucination* [35].

4.2. Implementation Details

We apply DyVTE to three popular MLLMs, namely Eagle-X5 7B [45], VILA 7B [37], InternVL [11], LLaVA-1.5 7B

[40] and LLaVA-1.5 13B [40]. Hyper-networks in the different layers do not share parameters. The scale α is set to 1.03 to filter out samples with large deviations in the generated distribution. For all MLLMs, the hidden dimension of the hyper-network is set to 2,048. During training, we freeze the original MLLMs, and the training rate of hyper-networks is set to 4×10^{-5} . And we randomly sample 1% from the training set of the 665k instruction data of LLaVA-1.5 [40] to train hyper-networks. The training epoch is set to 1. More details can refer to our code project.

4.3. Quantitative Analysis

4.3.1. Attention behaviors and visual redundancy

We first quantitatively investigate the attention behaviors of a set of MLLMs, and show that how the three main stages mentioned are summarized. Afterwards, we demonstrate the visual redundancy in the multimodal reasoning stage.

Attention behaviors of MLLMs. We first visualize the attention patterns of 4 MLLMs in Fig.3, including *visual self-attention*, *visual-text cross-attention* and *text self-attention*. Here, the values in these distributions are the averaged attention scores on the *LLaVA-split* [40], which can reflect the intensity of different attention modes. From these plots, we can first observe that four MLLMs share similar patterns for different types of attention. At the shallow layers, all MLLMs exhibit obvious cross-attention interactions between visual and text tokens, suggesting the intensive interactions between two modalities. This corresponds to the *early fusion* stage we termed above, which refers to the quick exchange of multimodal information. But this activity will quickly decline, and we can observe that the self-attention modeling within visual and text tokens becomes more active, *e.g.*, between two red lines. In this case, we can assume that MLLM focuses starts the *intra-modality modeling* stage. After that, the cross-attention gradually resumes and shows a certain degree of vibration. At the same time, the other attentions present relatively irregular trends. Here, we term this phase as the *multimodal reasoning* stage. Notably, we can find these patterns exists in four MLLMs of different families and scales.

The impact of dropping all visual tokens. Next, we estimate the visual redundancy of MLLMs given their inference patterns discussed above. In Fig.4, we present the results of removing visual tokens on LLaVA-1.5 7B and 13B for four benchmarks with different exiting strategies. From these plots, we can first observe that visual tokens are not always required throughout the entire process, especially the last stage. For instance, on GQA, removing all visual tokens at 24-th layer only has 0.5% and 0.6% performance drops for LLaVA-1.5 7B and 13B, receptively. Another finding is that the exit time of visual tokens is different for different tasks or examples. For instance, the optimal exit layer of SQA is earlier than that of TextVQA, *i.e.*, 16 *v.s.* 25, suggesting

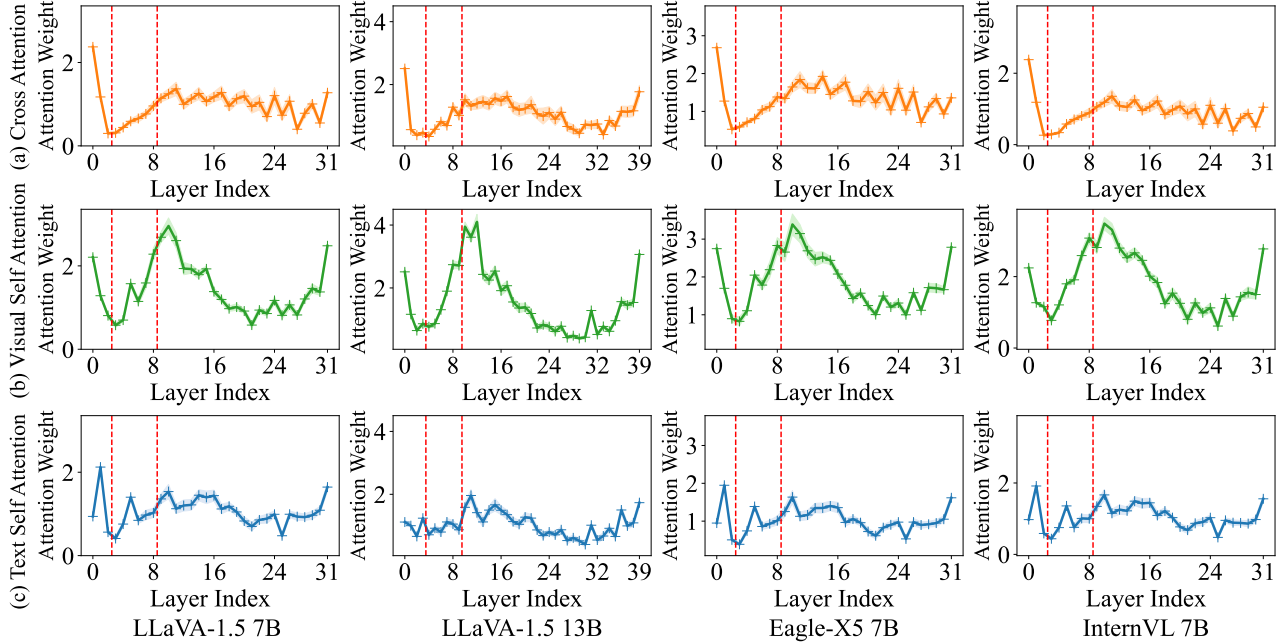


Figure 3. Distributions of averaged attention scores of image self-attention, cross-attention, and text self-attention. We visualize the mean and variance of the attention weight of each part on the LLaVA-1.5 7B, LLaVA-1.5 13B, Eagle-X5 7B and InternVL 7B. From these distributions, we can summarize three main stages of MLLMs as introduced in the main paper, which are then marked by red lines.

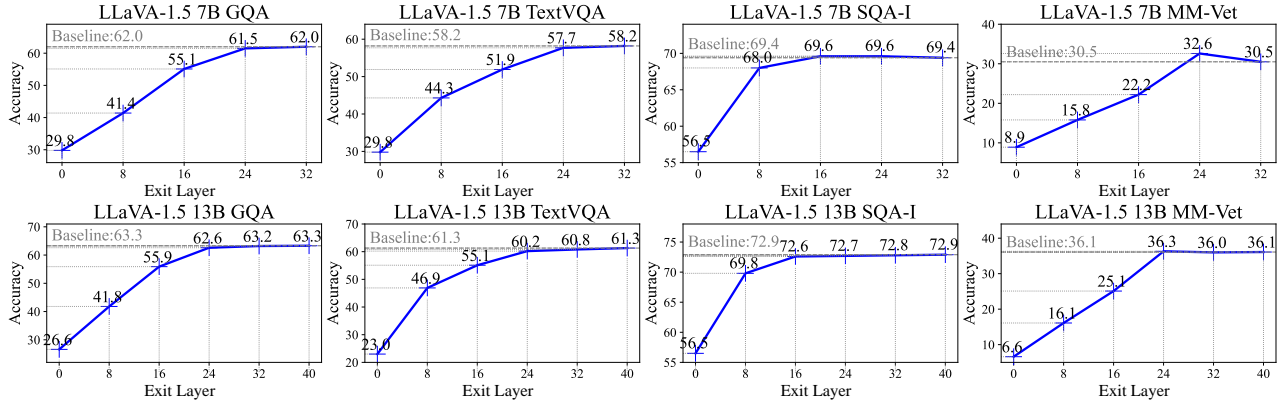


Figure 4. The relationship between manual visual-token exit and performance on LLaVA-1.5 7B and 13B. We show the results of removing all visual tokens at 0-th, 8-th, 16-th, 24-th and 32-th layers. “Baseline” represents the original performance of the MLLM. After a certain layer, the removal of all visual tokens barely impedes performance.

the need of DyVTER. More importantly, we can find that the correct removal of visual tokens has little impact on the self-attention patterns of text tokens. As shown in Fig.5, the text self-attention still presents similar distributions after using DyVTE, regardless of the self-modeling of visual tokens. The only difference lies in the slight change of attention intensity due to the shorter token sequence. Overall, these results well validate that visual tokens barely make contributions after a certain phase, and dynamically removing all visual tokens has little impact on the reasoning.

4.3.2. Results of DyVTE

The attention entropy with visual tokens exit. In Fig.5, we visualize the entropy distributions of cross-attention ma-

trices and text self-attention matrices of LLaVA-1.5 7B, and compare the results with and without DyVTE across four benchmarks. We first observe that the processes of multi-modal reasoning are generally similar across these benchmarks. In the text self-attention matrix, which is involved in answer generation, the entropy distributions across these datasets are quite similar. Another key observation is that visual tokens are often redundant in multimodal reasoning. Specifically, after removing all visual tokens, cross-modality information transfer is no longer performed, yet the text self-attention remains largely unaffected, as discussed above. Additionally, our DyVTE method can effectively remove all visual tokens at a specific layer according

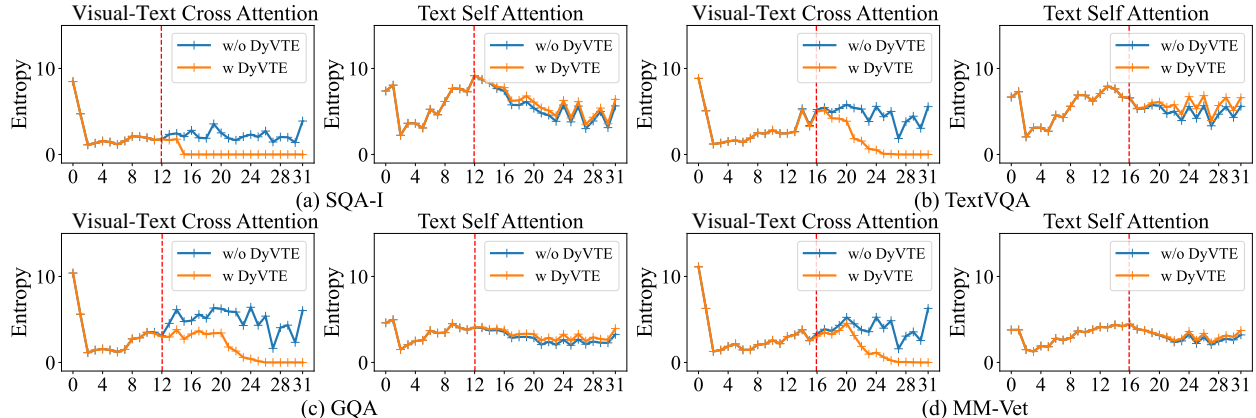


Figure 5. The entropy of two attention distributions. We visualize the entropy of cross-attention matrices and text self-attention on LLaVA-1.5 7B with and without our DyVTE, which shows that the removal of visual tokens barely affect the text self-attention.

Table 1. Results of MLLMs with and without DyVTE on five MLLM benchmarks. The accuracy (higher is better) and TFLOPs (lower is better) are reported. The relative percentage change from the baseline model to DyVTE is also shown in parentheses.

Method	SEED		MME		MMB		POPE		MM-Vet	
	Accuracy \uparrow	TFLOPs \downarrow	Score \uparrow	TFLOPs \downarrow	Accuracy \uparrow	TFLOPs \downarrow	Accuracy \uparrow	TFLOPs \downarrow	Accuracy \uparrow	TFLOPs \downarrow
Eagle-X5 7B [45]	73.9	47.8	1528.0	27.8	68.4	29.6	88.8	27.7	37.4	27.6
Eagle-DyVTE 7B	73.6 (-0.4%)	43.0 (-10.0%)	1581.7 (+3.5%)	20.3 (-27.0%)	68.8(+0.6%)	23.7 (-19.9%)	88.4 (-0.5%)	20.0 (-27.8%)	37.8 (+1.1%)	23.5 (-14.9%)
VILA 7B [37]	61.7	9.2	1489.2	8.9	69.9	9.5	86.3	8.8	36.3	8.7
VILA-DyVTE 7B	61.8 (+0.2%)	5.9 (-35.9%)	1503.1 (+0.1%)	4.6 (-48.3%)	69.8 (-0.1%)	6.0 (-36.8%)	85.6 (-0.8%)	4.5 (-48.9%)	36.7 (+1.1%)	6.6 (-24.1%)
InternVL 7B [11]	59.2	16.0	1525.1	15.5	64.6	16.2	86.4	15.4	31.2	15.4
Intern-DyVTE 7B	59.1 (-0.2%)	11.9 (-25.6%)	1474.1 (-3.3%)	10.9 (-29.7%)	64.4 (-0.3%)	12.0 (-25.9%)	81.3 (-5.9%)	10.9 (-29.2%)	29.5 (-5.4%)	13.0 (-15.6%)
LLaVA-1.5 7B [40]	58.6	9.2	1510.7	8.9	64.3	9.6	85.9	8.8	30.5	8.7
LLaVA-DyVTE 7B	58.6 (0.0%)	5.0 (-45.7%)	1491.4 (-1.3%)	6.3 (-29.2%)	64.7 (+0.6%)	5.4 (-43.8%)	81.6 (-5.0%)	4.1 (-53.4%)	31.9 (+4.6%)	6.3 (-27.6%)
LLaVA-1.5 13B [40]	61.6	17.6	1531.3	16.9	67.7	18.3	85.9	16.8	36.1	16.7
LLaVA-DyVTE 13B	59.3 (-3.7%)	7.1 (-59.7%)	1546.4 (+1.0%)	7.2 (-57.4%)	66.0 (-2.5%)	7.8 (-57.4%)	84.8 (-1.3%)	7.6 (-54.8%)	34.8 (-3.6%)	10.6 (-36.5%)

Table 2. Results of MLLMs with and without DyVTE on four VL benchmarks. The accuracy (higher is better) and TFLOPs (lower is better) are reported. The relative percentage change from the baseline model to DyVTE is also shown in parentheses.

Method	GQA		VQA		TextVQA		SQA-I		Average	
	Accuracy \uparrow	TFLOPs \downarrow	Score \uparrow	TFLOPs \downarrow	Accuracy \uparrow	TFLOPs \downarrow	Accuracy \uparrow	TFLOPs \downarrow	Accuracy \uparrow	TFLOPs \downarrow
Eagle-X5 7B [45]	64.9	27.8	83.4	27.8	71.2	29.5	69.8	29.2	72.3	28.6
Eagle-DyVTE 7B	62.4 (-3.9%)	21.7 (-21.9%)	82.6 (-1.0%)	21.6 (22.3%)	70.2 (-1.4%)	24.5 (-16.8%)	71.7 (+2.7%)	23.5 (-24.3%)	71.7 (-0.8%)	22.8 (-20.3%)
VILA 7B [37]	63.1	8.8	80.3	8.8	62.6	9.5	69.5	9.8	68.8	9.2
VILA-DyVTE 7B	61.9 (-1.9%)	5.5 (-37.5%)	79.2 (-1.4%)	5.4 (-38.6%)	61.2 (-2.2%)	7.2 (-24.2%)	69.5(0.0%)	6.1 (-37.8%)	67.9 (-1.3%)	6.0 (-34.8%)
InternVL 7B [11]	62.9	15.4	79.3	15.4	57.0	16.1	66.2	16.4	66.4	15.8
Intern-DyVTE 7B	61.3 (-2.5%)	11.8 (-23.4%)	77.6 (-2.1%)	11.7 (-24.0%)	55.8 (-2.1%)	13.5 (-16.1%)	66.2 (0.0%)	12.1 (-26.2%)	65.2 (-1.8%)	12.3 (-22.2%)
LLaVA-1.5 7B [40]	62.0	8.8	78.5	8.8	58.2	9.5	69.4	9.8	67.0	9.2
LLaVA-DyVTE 7B	60.0 (-3.2%)	5.3 (-39.8%)	76.6 (-2.4%)	5.1 (-42.0%)	56.6 (-2.7%)	6.7 (-29.5%)	69.6 (+0.3%)	5.5 (-43.9%)	65.7 (-1.9%)	5.6 (-39.1%)
LLaVA-1.5 13B [40]	63.3	16.8	80.0	16.8	61.3	18.1	72.9	18.6	69.4	17.6
LLaVA-DyVTE 13B	62.3 (-1.6%)	9.0 (-46.4%)	78.8 (-1.5%)	8.9 (-47.0%)	58.9 (-3.9%)	10.8 (-40.3%)	72.3 (-0.8%)	8.2 (-55.9%)	68.1 (-1.9%)	9.2 (-47.7%)

to the status of multimodal reasoning. In particular, the exit determined by DyVTE only blocks cross-modality information diffusion while preserving the modeling of text tokens. Overall, these findings support our motivation that visual tokens becomes redundant before the end of inference.

Results of DyVTE on different MLLMs. In Tab.1 and Tab.2, we present the results of applying DyVTE to a set of MLLMs of different families and sizes, including Eagle [45], VILA [37], InternVL [11], and LLaVA-1.5 [40]. From the tables, we can first observe that DyVTE significantly reduces computational overhead in existing MLLMs. For ex-

ample, LLaVA-DyVTE 7B achieves a 45.7% reduction in FLOPs on SEED without sacrificing performance. Additionally, the extent of FLOPs reduction varies depending on the task. On SQA with multiple-choice questions, DyVTE reduces computational overhead by up to 43.9%, while on the more detailed MM-Vet dataset, the reduction is 27.6%. Another notable observation is that DyVTE’s impact varies across different MLLMs. Specifically, VILA-DyVTE 7B reduces computational overhead by 48.3% on the MME benchmark with no performance drop, whereas LLaVA-DyVTE 7B only reduces overhead by 29.2%. When ap-

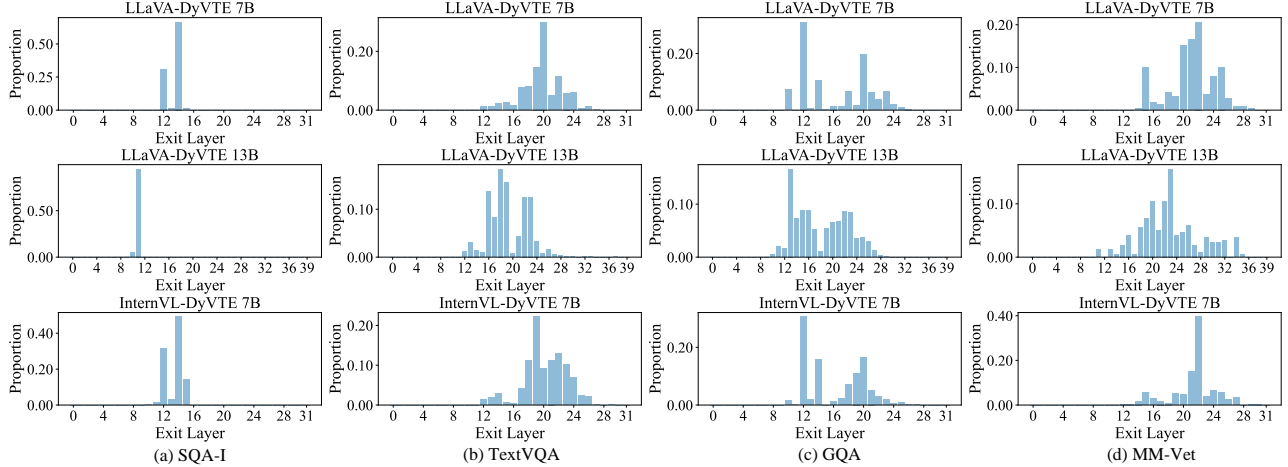


Figure 6. Statistics of the exiting layers decided by DyVTE on LLaVA-1.5 7B, LLaVA-1.5 13B and InternVL 7B. The horizontal axis represents the exit layer, and the vertical axis represents the proportion. The exit time by is different for different tasks, but similar for the MLLMs with the same sizes.

Table 3. Ablation study of the token status selection for DyVTE. “*Mean Visual*” denotes the average of all visual tokens except the last one, similar with “*Mean Text*”. “*Last Visual*” and “*Last Text*” denotes the last visual or text token. “*Exit Layer*” denotes the averaged layer numbers selected to remove by DyVTE. “*Acc.*” denotes the accuracy. The default setting of DyVTE is the last row. The best and second best results are marked in **bold** and underline, receptively.

State		GQA		TextVQA		MM-Vet		SQA-I		Average	
Mean Visual	Last Visual	Mean Text	Last Text	Acc. \uparrow	Exit Layer \downarrow						
✓				61.4	21.6	<u>57.3</u>	<u>21.0</u>	31.5	21.4	<u>69.7</u>	21.7
	✓			<u>61.2</u>	21.3	57.1	21.1	30.0	21.0	<u>69.7</u>	21.4
		✓		60.1	<u>17.4</u>	57.6	22.1	<u>31.1</u>	22.1	<u>69.7</u>	<u>20.4</u>
			✓	59.8	16.3	56.3	19.1	29.9	21.0	69.8	13.8
✓	✓			61.1	21.2	57.3	21.3	31.6	<u>21.3</u>	69.7	21.0
✓		✓		58.7	16.5	57.6	22.2	32.7	22.5	69.7	21.3
✓			✓	59.4	16.3	56.5	<u>19.9</u>	30.9	21.8	69.7	<u>14.4</u>
	✓	✓		59.4	16.7	<u>57.4</u>	21.8	31.3	22.0	69.6	20.3
		✓	✓	59.3	<u>16.4</u>	56.5	<u>19.9</u>	31.2	21.6	69.6	<u>14.4</u>
		✓	✓	<u>60.0</u>	<u>16.4</u>	56.6	19.7	<u>31.9</u>	21.1	69.6	13.4

plying DyVTE to larger MLLMs, such as LLaVA-1.5 13B, we can observe a more significant efficiency improvement, *i.e.*, LLaVA-DyVTE 13B reduces computational overhead by 55.9% on SQA, with only a 0.8% performance drop. Furthermore, DyVTE proves to be particularly effective for MLLMs with strong visual representations. For instance, when DyVTE is applied to Eagle-X5 7B, which has a visual encoder containing 13.3 TFLOPs, the performance drop is minimal, *i.e.* only 0.8% on traditional benchmarks, while Eagle-DyVTE 7B achieves a reduction of up to 6.2 TFLOPs in computational overhead.

The distribution of exit layers. In Fig. 6, we present the distributions of the visual token exit layers for LLaVA-DyVTE 7B and 13B. From the figure, we observe that DyVTE dynamically selects the exit layer based on the specific task requirements. For example, on the TextVQA dataset, which demands fine-grained information, the exit occurs later compared to other datasets. In contrast, on the

GQA dataset, which involves open-ended word questions and simple true/false judgments, the exit layers are more evenly distributed across early and late layers. Another notable observation is that the timing of the exit layer shows similar distributions across MLLMs of different scales and architectures. For instance, both LLaVA-DyVTE 7B and 13B remove all visual tokens at the same layer early in the process on the SQA dataset. Similarly, for InternVL and LLaVA, peaks in the exit layer distributions occur at comparable layers. Overall, these results support our motivation and the proposed DyVTE.

Ablation study. In Tab.3, we perform a set of experiments to analyze the impact of different representation selections on DyVTE. In this table, various tokens are used as the token status in Eq.1. As shown in Tab.3, when relying on image-only tokens, the model tends to remove all visual tokens at a later stage, specifically after the 21-st layer. Using the “*mean text*” token status allows for an earlier exit

Table 4. Comparison between DyVTE and token pruning methods. The best and second best results are marked in **bold** and underline.

Method	SQA-I		MM-Vet		SEED		MMB		Average	
	Accuracy \uparrow	TFLOPs \downarrow	Score \uparrow	TFLOPs \downarrow	Accuracy \uparrow	TFLOPs \downarrow	Accuracy \uparrow	TFLOPs \downarrow	Accuracy \uparrow	TFLOPs \downarrow
LLaVA[40]	69.4	9.8	30.5	8.7	58.6	9.2	64.3	9.6	55.7	9.3
ToMe [4]	69.6 (+0.3%)	5.9 (-39.8%)	30.6 (+0.3%)	<u>4.9</u> (-43.7%)	57.8 (-1.4%)	5.5 (-40.2%)	63.7 (-0.9%)	5.7 (-40.6%)	55.4 (-0.5%)	<u>5.5</u> (-40.9%)
FastV [8]	69.0 (-0.6%)	6.2 (-36.7%)	<u>31.3</u> (+2.6%)	5.2 (-35.8%)	<u>58.2</u> (-0.7%)	5.8 (-37.0%)	<u>64.4</u> (+0.2%)	6.0 (-37.5%)	<u>55.7</u> (0.0%)	5.8 (-37.6%)
DyVTE	69.6 (+0.3%)	<u>5.5</u> (-43.9%)	31.9 (+4.6%)	6.3 (-27.6%)	58.6 (0.0%)	<u>5.0</u> (-45.7%)	64.7 (+0.6%)	<u>5.4</u> (-43.8%)	56.2 (+0.9%)	<u>5.5</u> (-40.9%)
DyVTE+FastV	68.9 (-0.7%)	4.8 (-51.0%)	29.8 (-2.3%)	4.0 (-54.0%)	<u>58.2</u> (-0.7%)	4.6 (-50.0%)	<u>64.4</u> (+0.2%)	4.6 (-52.1%)	55.3 (-0.7%)	4.5 (-51.5%)

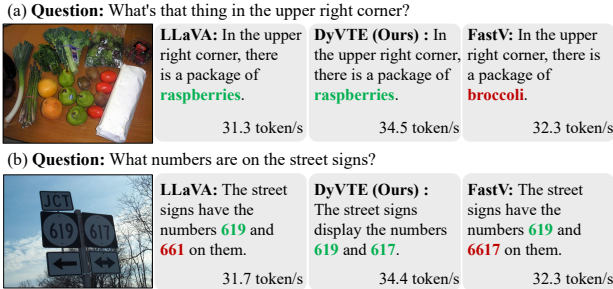


Figure 7. Examples on LLaVA-1.5 with DyVTE. Our DyVTE can help the MLLM answer the questions as accurately as default, while being faster, *i.e.*, more *tokens per second*.

from the layers. When only the “*last text*” token is used, DyVTE removes all visual tokens prematurely, *e.g.*, the 17-th layer, resulting in a more obvious performance drop of 1.0% on average. For combinations of two representations, we can observe that the “*mean text + last text*” is more effective. Specifically, it removes visual tokens at the about 17-th layer, while causing only a 0.5% performance drop. On the other hand, using a combination of visual token statuses, *i.e.*, “*mean Visual + last visual*”, yields results similar to using a single visual representation, with visual tokens being retained until the 21-st layer. Overall, these results well confirm the use of text token status for dynamic visual-token exiting in MLLMs.

Comparison with token pruning methods. In Tab.4, we compare the performance and efficiency of DyVTE with the visual token pruning methods of different principles. From the table, we can observe that DyVTE outperforms token pruning methods in both performance and efficiency. For example, when compared with ToMe on SQA, DyVTE not only maintains better performance but also reduces FLOPs by 4.1%. In comparison to FastV, the advantage of DyVTE can be more pronounced. Specifically, DyVTE improves performance while reducing computation overhead by 8.7% on the SEED benchmark. Another key observation is that DyVTE exhibits significant performance gains on more complex tasks. For instance, on the MM-Vet benchmark, which evaluates multiple capabilities including math and OCR, DyVTE improves performance by 4.3% compared to ToMe. Additionally, DyVTE demonstrates excellent compatibility with existing methods. When combined with FastV, DyVTE reduces computation over-

head by 51.5%, with only a 0.7% performance drop on average. Overall, these results validate the effectiveness and efficiency of DyVTE, establishing it as a powerful tool in efficient MLLM development.

4.4. Qualitative Analysis

To gain insight into the proposed DyVTE, we visualize its predictions and inference efficiency on LLaVA-1.5 7B in Fig.7. We can first observe that the implementation of DyVTE maintains consistency with the default LLaVA. As shown in Fig.7-(a), DyVTE can correctly identify the object in question, even with a complex foreground. Additionally, it is clear that DyVTE provides much faster inference than the default LLaVA. For two examples, DyVTE can improve the inference speed by up to 10.2% compared to the default LLaVA. Another observation is that removing redundant visual information can further enhance the LLaVA’s performance. As shown in Fig.7-(b), similar to the results on the MM-Vet benchmark, removing visual tokens also improves the performance of the default LLaVA. Overall, these results confirm that DyVTE enhances inference efficiency without compromising the reasoning process of the default model, aligning well with our motivation.

5. Conclusion

In this paper, we investigate the attention patterns in *multimodal large language models* (MLLMs) and propose a simple yet effective method, *dynamic visual-token exit* (DyVTE), to improve computational efficiency. By analyzing the attention patterns in the MLLMs, we identify three key stages of most MLLMs in the attention process, *i.e.*, *early fusion*, *inter-modality modeling*, and *multimodal reasoning*. Based on this finding, we further show that visual tokens contribute less to the reasoning process as inference progresses. Motivated by this insight, DyVTE optimally determines the layer at which visual tokens can be removed, thereby reducing computational overhead without compromising performance. Extensive experiments across five MLLMs and VL benchmark benchmarks demonstrate that DyVTE significantly enhances the efficiency of MLLMs while maintaining their performance.

6. Acknowledgments

This work was supported by National Science and Technology Major Project (No. 2022ZD0118201), the National Science Fund for Distinguished Young Scholars (No.62025603), the National Natural Science Foundation of China (No. U21B2037, No. U22B2051, No. U23A20383, No. U21A20472, No. 62176222, No. 62176223, No. 62176226, No. 62072386, No. 62072387, No. 62072389, No. 62002305 and No. 62272401), and the Natural Science Foundation of Fujian Province of China (No. 2021J06003, No.2022J06001).

References

- [1] Josh Achiam, Steven Adler, Sandhini Agarwal, Lama Ahmad, Ilge Akkaya, Florencia Leoni Aleman, Diogo Almeida, Janko Altenschmidt, Sam Altman, Shyamal Anadkat, et al. Gpt-4 technical report. *arXiv preprint arXiv:2303.08774*, 2023. 1, 2
- [2] Jinze Bai, Shuai Bai, Yunfei Chu, Zeyu Cui, Kai Dang, Xiaodong Deng, Yang Fan, Wenbin Ge, Yu Han, Fei Huang, et al. Qwen technical report. *arXiv preprint arXiv:2309.16609*, 2023. 1, 2
- [3] Jinze Bai, Shuai Bai, Shusheng Yang, Shijie Wang, Sinan Tan, Peng Wang, Junyang Lin, Chang Zhou, and Jingren Zhou. Qwen-vl: A frontier large vision-language model with versatile abilities. *arXiv preprint arXiv:2308.12966*, 2023. 1, 2
- [4] Daniel Bolya, Cheng-Yang Fu, Xiaoliang Dai, Peizhao Zhang, Christoph Feichtenhofer, and Judy Hoffman. Token merging: Your vit but faster. *arXiv preprint arXiv:2210.09461*, 2022. 2, 8
- [5] Daniel Bolya, Cheng-Yang Fu, Xiaoliang Dai, Peizhao Zhang, Christoph Feichtenhofer, and Judy Hoffman. Token merging: Your vit but faster. *arXiv preprint arXiv:2210.09461*, 2022. 3
- [6] Tom B Brown. Language models are few-shot learners. *arXiv preprint arXiv:2005.14165*, 2020. 1
- [7] Jianjian Cao, Peng Ye, Shengze Li, Chong Yu, Yansong Tang, Jiwen Lu, and Tao Chen. Madtp: Multimodal alignment-guided dynamic token pruning for accelerating vision-language transformer. In *Proceedings of the IEEE/CVF Conference on Computer Vision and Pattern Recognition*, pages 15710–15719, 2024. 1
- [8] Liang Chen, Haozhe Zhao, Tianyu Liu, Shuai Bai, Junyang Lin, Chang Zhou, and Baobao Chang. An image is worth 1/2 tokens after layer 2: Plug-and-play inference acceleration for large vision-language models. *arXiv preprint arXiv:2403.06764*, 2024. 2, 3, 8
- [9] Mengzhao Chen, Wenqi Shao, Peng Xu, Mingbao Lin, Kaipeng Zhang, Fei Chao, Rongrong Ji, Yu Qiao, and Ping Luo. Difftrate: Differentiable compression rate for efficient vision transformers. In *Proceedings of the IEEE/CVF International Conference on Computer Vision*, pages 17164–17174, 2023. 1
- [10] Yanxi Chen, Xuchen Pan, Yaliang Li, Bolin Ding, and Jingren Zhou. Ee-llm: Large-scale training and inference of early-exit large language models with 3d parallelism. *arXiv preprint arXiv:2312.04916*, 2023. 2, 3
- [11] Zhe Chen, Jiannan Wu, Wenhai Wang, Weijie Su, Guo Chen, Sen Xing, Muyan Zhong, Qinglong Zhang, Xizhou Zhu, Lewei Lu, Bin Li, Ping Luo, Tong Lu, Yu Qiao, and Jifeng Dai. Internvl: Scaling up vision foundation models and aligning for generic visual-linguistic tasks. *arXiv preprint arXiv:2312.14238*, 2023. 2, 4, 6
- [12] Zhe Chen, Weiyun Wang, Hao Tian, Shenglong Ye, Zhangwei Gao, Erfei Cui, Wenwen Tong, Kongzhi Hu, Jiapeng Luo, Zheng Ma, et al. How far are we to gpt-4v? closing the gap to commercial multimodal models with open-source suites. *arXiv preprint arXiv:2404.16821*, 2024. 1, 2
- [13] Tri Dao, Dan Fu, Stefano Ermon, Atri Rudra, and Christopher Ré. Flashattention: Fast and memory-efficient exact attention with io-awareness. *Advances in Neural Information Processing Systems*, 35:16344–16359, 2022. 2
- [14] Luciano Del Corro, Allie Del Giorno, Sahaj Agarwal, Bin Yu, Ahmed Awadallah, and Subhabrata Mukherjee. Skipdecode: Autoregressive skip decoding with batching and caching for efficient llm inference. *arXiv preprint arXiv:2307.02628*, 2023. 3
- [15] Jacob Devlin. Bert: Pre-training of deep bidirectional transformers for language understanding. *arXiv preprint arXiv:1810.04805*, 2018. 3
- [16] Peiyan Dong, Mengshu Sun, Alec Lu, Yanyue Xie, Kenneth Liu, Zhenglun Kong, Xin Meng, Zhengang Li, Xue Lin, Zhenman Fang, et al. Heatvit: Hardware-efficient adaptive token pruning for vision transformers. In *2023 IEEE International Symposium on High-Performance Computer Architecture (HPCA)*, pages 442–455. IEEE, 2023. 1, 3
- [17] Xiaoyi Dong, Pan Zhang, Yuhang Zang, Yuhang Cao, Bin Wang, Linke Ouyang, Xilin Wei, Songyang Zhang, Haodong Duan, Maosong Cao, et al. Internlm-xcomposer2: Mastering free-form text-image composition and comprehension in vision-language large model. *arXiv preprint arXiv:2401.16420*, 2024. 2
- [18] Alexey Dosovitskiy. An image is worth 16x16 words: Transformers for image recognition at scale. *arXiv preprint arXiv:2010.11929*, 2020. 3
- [19] Abhimanyu Dubey, Abhinav Jauhri, Abhinav Pandey, Abhishek Kadian, Ahmad Al-Dahle, Aiesha Letman, Akhil Mathur, Alan Schelten, Amy Yang, Angela Fan, et al. The llama 3 herd of models. *arXiv preprint arXiv:2407.21783*, 2024. 1, 2
- [20] Mostafa Elhoushi, Akshat Shrivastava, Diana Liskovich, Basil Hosmer, Bram Wasti, Liangzhen Lai, Anas Mahmoud, Bilge Acun, Saurabh Agarwal, Ahmed Roman, et al. Layer skip: Enabling early exit inference and self-speculative decoding. *arXiv preprint arXiv:2404.16710*, 2024. 3
- [21] Siqi Fan, Xin Jiang, Xiang Li, Xuying Meng, Peng Han, Shuo Shang, Aixin Sun, Yequan Wang, and Zhongyuan Wang. Not all layers of llms are necessary during inference. *arXiv preprint arXiv:2403.02181*, 2024. 2, 3
- [22] Mohsen Fayyaz, Soroush Abbasi Koohpayegani, Farnoush Rezaei Jafari, Sunando Sengupta, Hamid Reza Vaezi Joze, Eric Sommerlade, Hamed Pirsiavash, and

- Jürgen Gall. Adaptive token sampling for efficient vision transformers. In *European Conference on Computer Vision*, pages 396–414. Springer, 2022. 3
- [23] William Fedus, Barret Zoph, and Noam Shazeer. Switch transformers: Scaling to trillion parameter models with simple and efficient sparsity. *Journal of Machine Learning Research*, 23(120):1–39, 2022. 3
- [24] Chaoyou Fu, Peixian Chen, Yunhang Shen, Yulei Qin, Mengdan Zhang, Xu Lin, Jinrui Yang, Xiawu Zheng, Ke Li, Xing Sun, Yunsheng Wu, and Rongrong Ji. Mme: A comprehensive evaluation benchmark for multimodal large language models. *Computing Research Repository (CoRR)*, 2023. 2, 4
- [25] Amir Ghodrati, Babak Ehteshami Bejnordi, and Amirhossein Habibi. Frameexit: Conditional early exiting for efficient video recognition. In *Proceedings of the IEEE/CVF Conference on Computer Vision and Pattern Recognition*, pages 15608–15618, 2021. 2
- [26] Yash Goyal, Tejas Khot, Douglas Summers-Stay, Dhruv Batra, and Devi Parikh. Making the v in vqa matter: Elevating the role of image understanding in visual question answering. In *Proceedings of the IEEE conference on computer vision and pattern recognition*, pages 6904–6913, 2017. 2, 4
- [27] Drew A Hudson and Christopher D Manning. Gqa: A new dataset for real-world visual reasoning and compositional question answering. In *CVPR*, 2019. 2, 4
- [28] Albert Q Jiang, Alexandre Sablayrolles, Antoine Roux, Arthur Mensch, Blanche Savary, Chris Bamford, Devendra Singh Chaplot, Diego de las Casas, Emma Bou Hanna, Florian Bressand, et al. Mixtral of experts. *arXiv preprint arXiv:2401.04088*, 2024. 1, 2
- [29] Sehoon Kim, Sheng Shen, David Thorsley, Amir Gholami, Woosuk Kwon, Joseph Hassoun, and Kurt Keutzer. Learned token pruning for transformers. In *Proceedings of the 28th ACM SIGKDD Conference on Knowledge Discovery and Data Mining*, pages 784–794, 2022. 3
- [30] Zhenglun Kong, Peiyan Dong, Xiaolong Ma, Xin Meng, Wei Niu, Mengshu Sun, Xuan Shen, Geng Yuan, Bin Ren, Hao Tang, et al. Spvit: Enabling faster vision transformers via latency-aware soft token pruning. In *European conference on computer vision*, pages 620–640. Springer, 2022. 3
- [31] Solomon Kullback and Richard A Leibler. On information and sufficiency. *The annals of mathematical statistics*, 22(1): 79–86, 1951. 3
- [32] Bohao Li, Rui Wang, Guangzhi Wang, Yuying Ge, Yixiao Ge, and Ying Shan. Seed-bench: Benchmarking multimodal llms with generative comprehension. *Computing Research Repository (CoRR)*, 2023. 4
- [33] Bo Li, Yuanhan Zhang, Dong Guo, Renrui Zhang, Feng Li, Hao Zhang, Kaichen Zhang, Yanwei Li, Ziwei Liu, and Chunyuan Li. Llava-onevision: Easy visual task transfer. *arXiv preprint arXiv:2408.03326*, 2024. 1, 2
- [34] Junnan Li, Dongxu Li, Silvio Savarese, and Steven Hoi. Blip-2: Bootstrapping language-image pre-training with frozen image encoders and large language models. In *International conference on machine learning*, pages 19730–19742. PMLR, 2023. 2
- [35] Yifan Li, Yifan Du, Kun Zhou, Jinpeng Wang, Wayne Xin Zhao, and Ji-Rong Wen. Evaluating object hallucination in large vision-language models. *Computing Research Repository (CoRR)*, 2023. 2, 4
- [36] Bin Lin, Zhenyu Tang, Yang Ye, Jiayi Cui, Bin Zhu, Peng Jin, Jinfa Huang, Junwu Zhang, Yatian Pang, Munan Ning, et al. Moe-llava: Mixture of experts for large vision-language models. *arXiv preprint arXiv:2401.15947*, 2024. 3
- [37] Ji Lin, Hongxu Yin, Wei Ping, Yao Lu, Pavlo Molchanov, Andrew Tao, Huizi Mao, Jan Kautz, Mohammad Shoeybi, and Song Han. Vila: On pre-training for visual language models. *arXiv preprint arXiv:2312.07533*, 2023. 2, 4, 6
- [38] Daria Lioubashevski, Tomer Schlamk, Gabriel Stanovsky, and Ariel Goldstein. Looking beyond the top-1: Transformers determine top tokens in order. *arXiv preprint arXiv:2410.20210*, 2024. 3
- [39] Daria Lioubashevski, Tomer Schlamk, Gabriel Stanovsky, and Ariel Goldstein. Looking beyond the top-1: Transformers determine top tokens in order. *arXiv preprint arXiv:2410.20210*, 2024. 3
- [40] Haotian Liu, Chunyuan Li, Qingyang Wu, and Yong Jae Lee. Visual instruction tuning. *Advances in neural information processing systems*, 36, 2024. 1, 2, 4, 6, 8
- [41] Yuan Liu, Haodong Duan, Yuanhan Zhang, Bo Li, Songyang Zhang, Wangbo Zhao, Yike Yuan, Jiaqi Wang, Conghui He, Ziwei Liu, et al. Mmbench: Is your multi-modal model an all-around player? *Computing Research Repository (CoRR)*, 2023. 1, 2, 4
- [42] Pan Lu, Swaroop Mishra, Tanglin Xia, Liang Qiu, Kai-Wei Chang, Song-Chun Zhu, Oyvind Tafjord, Peter Clark, and Ashwin Kalyan. Learn to explain: Multimodal reasoning via thought chains for science question answering. *Advances in Neural Information Processing Systems*, 2022. 1, 4
- [43] Lingchen Meng, Hengduo Li, Bor-Chun Chen, Shiyi Lan, Zuxuan Wu, Yu-Gang Jiang, and Ser-Nam Lim. Adavit: Adaptive vision transformers for efficient image recognition. In *Proceedings of the IEEE/CVF Conference on Computer Vision and Pattern Recognition*, pages 12309–12318, 2022. 3
- [44] Yongming Rao, Wenliang Zhao, Benlin Liu, Jiwen Lu, Jie Zhou, and Cho-Jui Hsieh. Dynamicvit: Efficient vision transformers with dynamic token sparsification. *Advances in neural information processing systems*, 34:13937–13949, 2021. 3
- [45] Min Shi, Fuxiao Liu, Shihao Wang, Shijia Liao, Subhashree Radhakrishnan, De-An Huang, Hongxu Yin, Karan Sapra, Yaser Yacoob, Humphrey Shi, et al. Eagle: Exploring the design space for multimodal llms with mixture of encoders. *arXiv preprint arXiv:2408.15998*, 2024. 1, 2, 4, 6
- [46] Amanpreet Singh, Vivek Natarajan, Meet Shah, Yu Jiang, Xinlei Chen, Dhruv Batra, Devi Parikh, and Marcus Rohrbach. Towards vqa models that can read. In *Proceedings of the IEEE/CVF conference on computer vision and pattern recognition*, pages 8317–8326, 2019. 1, 2, 4
- [47] Alessandro Stolfo, Yonatan Belinkov, and Mrinmaya Sachan. A mechanistic interpretation of arithmetic reasoning

- in language models using causal mediation analysis. *arXiv preprint arXiv:2305.15054*, 2023. 3
- [48] Shengkun Tang, Yaqing Wang, Zhenglun Kong, Tianchi Zhang, Yao Li, Caiwen Ding, Yanzhi Wang, Yi Liang, and Dongkuan Xu. You need multiple exiting: Dynamic early exiting for accelerating unified vision language model. In *Proceedings of the IEEE/CVF Conference on Computer Vision and Pattern Recognition*, pages 10781–10791, 2023. 2
- [49] Qwen Team. Qwen2.5: A party of foundation models, 2024. 1
- [50] Hugo Touvron, Louis Martin, Kevin Stone, Peter Albert, Amjad Almahairi, Yasmine Babaei, Nikolay Bashlykov, Soumya Batra, Prajjwal Bhargava, Shruti Bhosale, et al. Llama 2: Open foundation and fine-tuned chat models. *arXiv preprint arXiv:2307.09288*, 2023. 1
- [51] A Vaswani. Attention is all you need. *Advances in Neural Information Processing Systems*, 2017. 3
- [52] Hongjie Wang, Bhishma Dedhia, and Niraj K Jha. Zero-prune: Zero-shot token pruning through leveraging of the attention graph in pre-trained transformers. In *Proceedings of the IEEE/CVF Conference on Computer Vision and Pattern Recognition*, pages 16070–16079, 2024. 1, 3
- [53] Peng Wang, Shuai Bai, Sinan Tan, Shijie Wang, Zhihao Fan, Jinze Bai, Keqin Chen, Xuejing Liu, Jialin Wang, Wenbin Ge, et al. Qwen2-vl: Enhancing vision-language model’s perception of the world at any resolution. *arXiv preprint arXiv:2409.12191*, 2024. 1, 2
- [54] Siyuan Wei, Tianzhu Ye, Shen Zhang, Yao Tang, and Jiajun Liang. Joint token pruning and squeezing towards more aggressive compression of vision transformers. In *Proceedings of the IEEE/CVF Conference on Computer Vision and Pattern Recognition*, pages 2092–2101, 2023. 1, 3
- [55] Qiong Wu, Zhaoxi Ke, Yiyi Zhou, Gen Luo, Xiaoshuai Sun, and Rongrong Ji. Routing experts: Learning to route dynamic experts in multi-modal large language models. *arXiv preprint arXiv:2407.14093*, 2024. 3
- [56] Qiong Wu, Wei Yu, Yiyi Zhou, Shubin Huang, Xiaoshuai Sun, and Rongrong Ji. Parameter and computation efficient transfer learning for vision-language pre-trained models. *Advances in Neural Information Processing Systems*, 36, 2024. 3
- [57] An Yang, Baosong Yang, Binyuan Hui, Bo Zheng, Bowen Yu, Chang Zhou, Chengpeng Li, Chengyuan Li, Dayiheng Liu, Fei Huang, Guanting Dong, Haoran Wei, Huan Lin, Jialong Tang, Jialin Wang, Jian Yang, Jianhong Tu, Jianwei Zhang, Jianxin Ma, Jin Xu, Jingren Zhou, Jinze Bai, Jinzheng He, Junyang Lin, Kai Dang, Keming Lu, Keqin Chen, Kexin Yang, Mei Li, Mingfeng Xue, Na Ni, Pei Zhang, Peng Wang, Ru Peng, Rui Men, Ruize Gao, Runji Lin, Shijie Wang, Shuai Bai, Sinan Tan, Tianhang Zhu, Tianhao Li, Tianyu Liu, Wenbin Ge, Xiaodong Deng, Xiaohuan Zhou, Xingzhang Ren, Xinyu Zhang, Xipin Wei, Xuancheng Ren, Yang Fan, Yang Yao, Yichang Zhang, Yu Wan, Yunfei Chu, Yuqiong Liu, Zeyu Cui, Zhenru Zhang, and Zhihao Fan. Qwen2 technical report. *arXiv preprint arXiv:2407.10671*, 2024. 1
- [58] Deming Ye, Yankai Lin, Yufei Huang, and Maosong Sun. Tr-bert: Dynamic token reduction for accelerating bert inference. In *Proceedings of the 2021 Conference of the North American Chapter of the Association for Computational Linguistics: Human Language Technologies*, pages 5798–5809, 2021. 3
- [59] Weihao Ye, Qiong Wu, Wenhao Lin, and Yiyi Zhou. Fit and prune: Fast and training-free visual token pruning for multi-modal large language models. *arXiv preprint arXiv:2409.10197*, 2024. 1, 3
- [60] Weihao Yu, Zhengyuan Yang, Linjie Li, Jianfeng Wang, Kevin Lin, Zicheng Liu, Xinchao Wang, and Lijuan Wang. Mm-vet: Evaluating large multimodal models for integrated capabilities. *Computing Research Repository (CoRR)*, 2023. 1, 2, 4
- [61] Ted Zadori, Ahmet Üstün, Arash Ahmadian, Beyza Ermiş, Acyr Locatelli, and Sara Hooker. Pushing mixture of experts to the limit: Extremely parameter efficient moe for instruction tuning. *arXiv preprint arXiv:2309.05444*, 2023. 3

Table 5. Ablation study of the token status selection for DyVTE. “*Mean Visual*” denotes the average of all visual tokens except the last one, similar with “*Mean Text*”. “*Last Visual*” and “*Last Text*” denotes the last visual or text token. “*Exit Layer*” denotes the averaged layer numbers selected to remove by DyVTE. “*Acc.*” denotes the accuracy. The default setting of DyVTE is the last row. The best and second best results are marked in **bold** and underline, receptively.

State		GQA		TextVQA		MM-Vet		SQA-I		Average			
Mean Visual	Last Visual	Mean Text	Last Text	Acc. ↑	Exit Layer ↓								
✓				61.4	21.6	<u>57.3</u>	<u>21.0</u>	31.5	21.4	<u>69.7</u>	21.7	55.0	21.4
	✓			<u>61.2</u>	21.3	57.1	21.1	30.0	21.0	<u>69.7</u>	21.4	54.5	21.2
		✓		60.1	<u>17.4</u>	57.6	22.1	<u>31.1</u>	22.1	<u>69.7</u>	<u>20.4</u>	<u>54.6</u>	<u>20.5</u>
			✓	59.8	16.3	56.3	19.1	29.9	21.0	69.8	13.8	54.0	17.6
✓	✓			61.1	21.2	57.3	21.3	31.6	<u>21.3</u>	69.7	21.0	54.9	21.2
✓		✓		58.7	16.5	57.6	22.2	32.7	22.5	69.7	21.3	<u>54.7</u>	20.6
✓			✓	59.4	16.3	56.5	<u>19.9</u>	30.9	21.8	69.7	<u>14.4</u>	54.1	<u>18.1</u>
	✓	✓		59.4	16.7	<u>57.4</u>	21.8	31.3	22.0	69.6	20.3	54.4	20.2
	✓		✓	59.3	<u>16.4</u>	56.5	<u>19.9</u>	31.2	21.6	69.6	<u>14.4</u>	54.1	<u>18.1</u>
		✓	✓	<u>60.0</u>	<u>16.4</u>	56.6	19.7	<u>31.9</u>	21.1	69.6	13.4	54.5	17.6
	✓	✓	✓	<u>60.1</u>	16.4	57.0	<u>20.2</u>	30.8	21.3	69.6	<u>14.1</u>	<u>54.4</u>	<u>18.0</u>
✓		✓	✓	60.2	16.7	<u>57.1</u>	20.3	<u>31.0</u>	<u>21.6</u>	69.7	14.3	54.5	18.2
✓	✓		✓	57.6	<u>15.9</u>	57.3	22.2	31.7	22.1	69.7	20.1	54.1	20.2
✓	✓	✓		57.8	15.2	56.2	19.3	30.0	<u>21.6</u>	69.3	11.7	53.3	16.9
✓	✓	✓	✓	60.5	16.8	57.1	20.5	31.1	21.8	69.8	14.1	54.6	18.3
LLaVA-1.5 7B				62.0	-	58.2	-	30.5	-	69.4	-	55.0	-

Table 6. Ablation study of the attention status selection for DyVTE. “*Visual Self*” denotes the attention score from visual modality of each visual tokens, similar with “*Text Self*”. “*Cross*” denotes the attention score from visual to the text of each visual tokens. For attention representations whose dimensions are not 576, we use interpolation to align the dimensions. “*Exit Layer*” denotes the averaged layer numbers selected to remove by DyVTE. “*Acc.*” denotes the accuracy. The default setting of DyVTE is the last row. The best and second best results are marked in **bold** and underline, receptively.

State			GQA		TextVQA		MM-Vet		SQA-I		Average	
Visual Self	Cross	Text Self	Acc. ↑	Exit Layer ↓								
✓			38.3	0.5	42.4	0.7	12.2	0.9	64.2	0.6	39.9	0.7
	✓		38.8	1.3	43.1	1.3	11.5	1.2	65.2	1.2	39.6	1.2
		✓	39.6	1.7	42.7	1.1	11.9	3.6	64.7	0.6	39.7	1.7
✓	✓		39.4	2.7	43.1	3.0	13.1	2.6	65.4	3.8	40.3	3.0
✓		✓	40.7	3.0	43.0	1.7	13.3	5.9	65.1	1.0	40.5	2.9
	✓	✓	40.7	3.0	43.1	1.6	13.4	6.0	65.2	1.0	40.6	2.9
✓	✓	✓	49.5	10.9	45.6	5.6	15.6	7.1	65.6	2.5	44.1	6.5
LLaVA-1.5 7B			62.0	-	58.2	-	30.5	-	69.4	-	55.0	-

A. Appendix

In this paper, we first conduct extensive empirical studies on the attention behaviors of MLLMs, and summarize three main inference stages in MLLMs: (i) *Early fusion* between tokens is first accomplished quickly. (ii) *Intra-modality modeling* then comes to play. (iii) *Multimodal reasoning* resumes and lasts until the end of inference. To better confirm our findings, we conduct further experiments on more MLLMs in the supplementary materials.

A.1. Ablation Study

In Tab.5 and Tab.6, we perform a set experiment to analyze the impact of different representation selections on DyVTE. As shown in Tab.5, when relying on more than two representations, we can find out that their performance is similar to “*mean text + last text*”. For instance, the additional representation, i.e., “*last visual*” and “*mean visual*”, has no noticeable effect on the results. We can also observe that the missing of “*mean text*” or “*last text*” will lead to inaccurate exit. For example, the missing of “*mean text*” leads to later exit, i.e., 2 layers latter, while the absence of “*last text*” does the opposite, i.e., 2 layers earlier. As for taking attention scores be the representations, we find that hyper-network can not make the correct judgment. Specifically, the exit layers for all benchmarks can be much earlier. Overall, these results well confirm the use of text tokens status for dynamic visual token exiting in MLLMs.

A.2. Distribution of Attention

In Fig 8-12, we further visualize the attention distributions on different MLLMs for different datasets. We can first observe that datasets produce similar attention patterns on the same MLLM. Another observation is that attention patterns across different MLLMs have similar trends and the distributions can generally be categorized into three distinct stages. These findings emphasize the universality of attention behavior in MLLMs, further validating our approach. Overall, the experiment results confirm that different MLLMs have similar attention patterns on the different data.

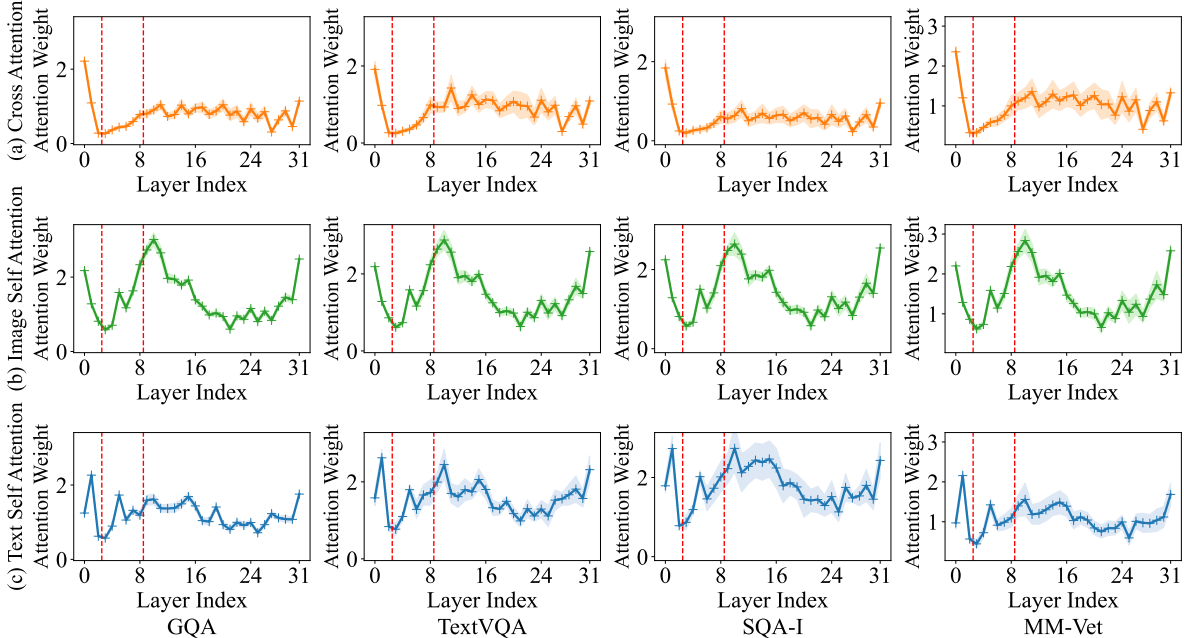


Figure 8. Distributions of averaged attention scores of image self-attention, cross-attention, and text self-attention of LLaVA-1.5 7B. We visualize the mean and variance of the attention weight of each part on GQA, TextVQA, SQA-I, MM-Vet datasets. From these distributions, we can summarize three main stages of MLLMs as introduced in the main paper, which are then marked by red lines.

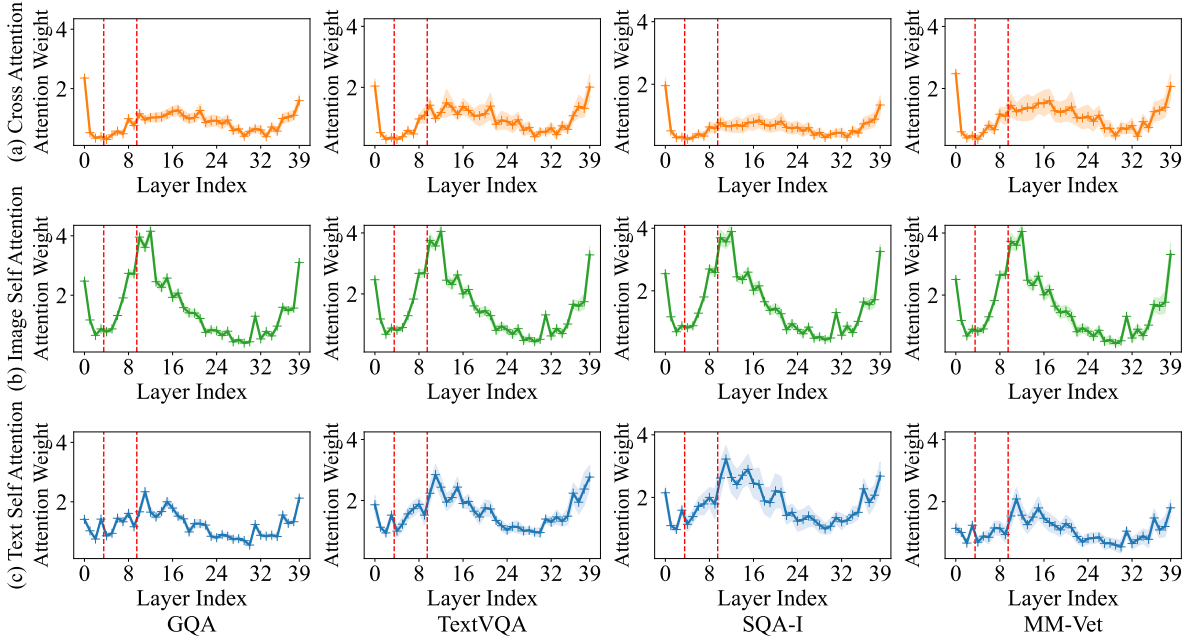


Figure 9. Distributions of averaged attention scores of image self-attention, cross-attention and text self-attention of LLaVA-1.5 13B. We visualize the mean and variance of the attention weight of each part on GQA, TextVQA, SQA-I, MM-Vet datasets. From these distributions, we can summarize three main stages of MLLMs as introduced in the main paper, which are then marked by red lines.

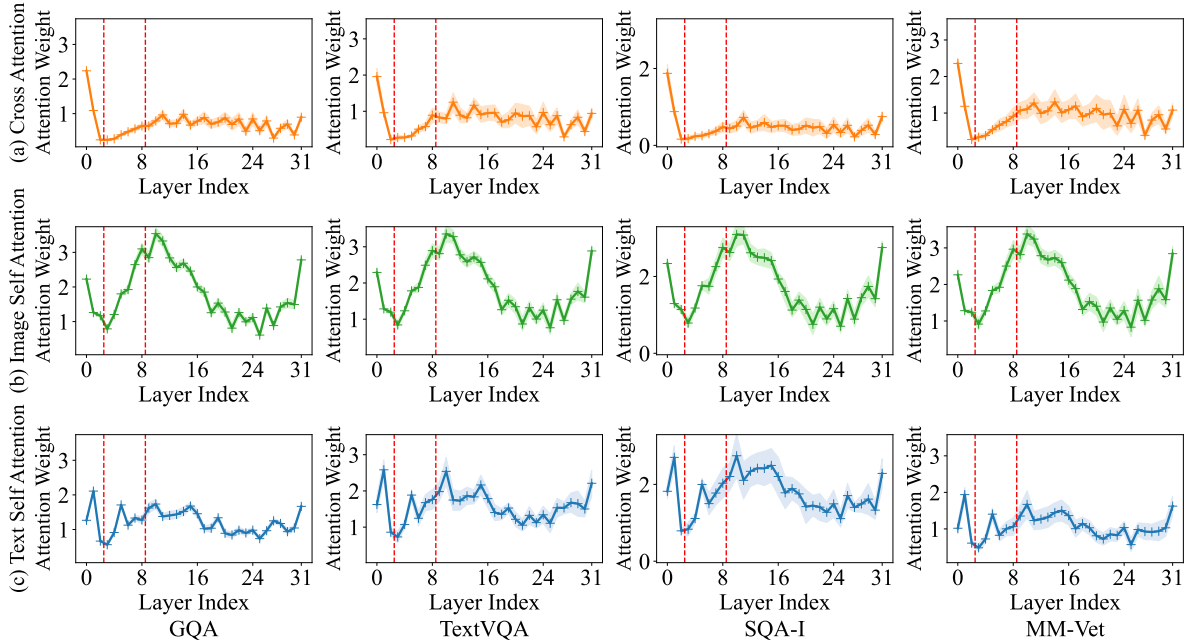


Figure 10. Distributions of averaged attention scores of image self-attention, cross-attention and text self-attention of InternVL 7B. We visualize the mean and variance of the attention weight of each part on GQA, TextVQA, SQA-I, MM-Vet datasets. From these distributions, we can summarize three main stages of MLLMs as introduced in the main paper, which are then marked by red lines.

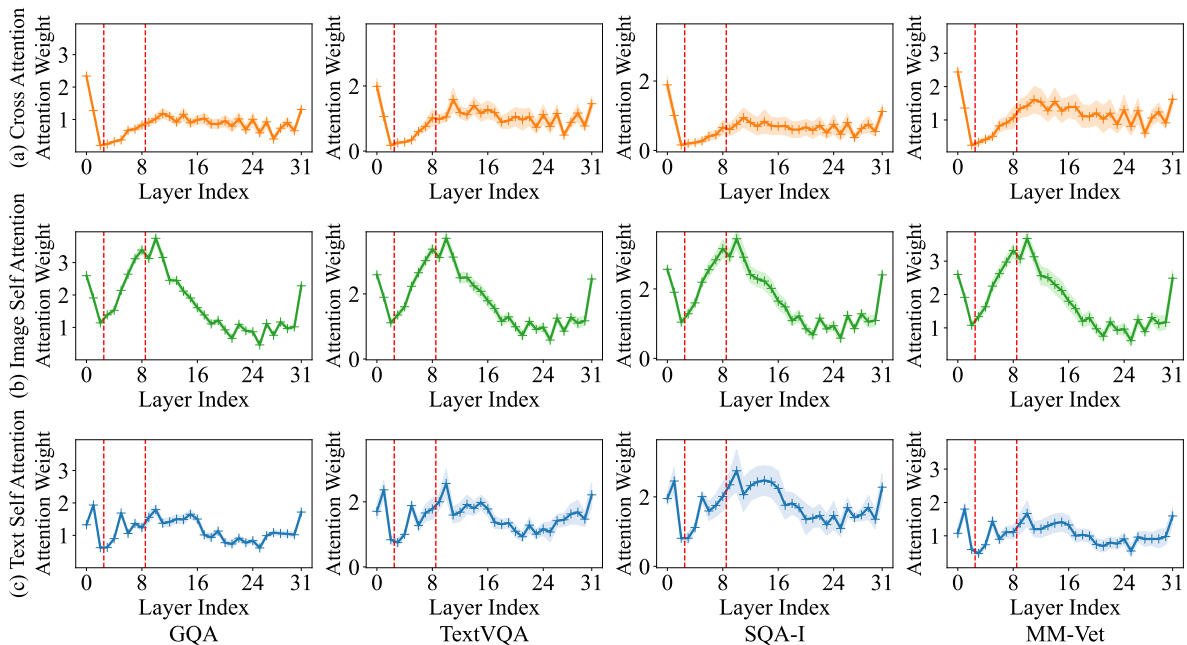


Figure 11. Distributions of averaged attention scores of image self-attention, cross-attention and text self-attention of VILA 7B. We visualize the mean and variance of the attention weight of each part on GQA, TextVQA, SQA-I, MM-Vet datasets. From these distributions, we can summarize three main stages of MLLMs as introduced in the main paper, which are then marked by red lines.

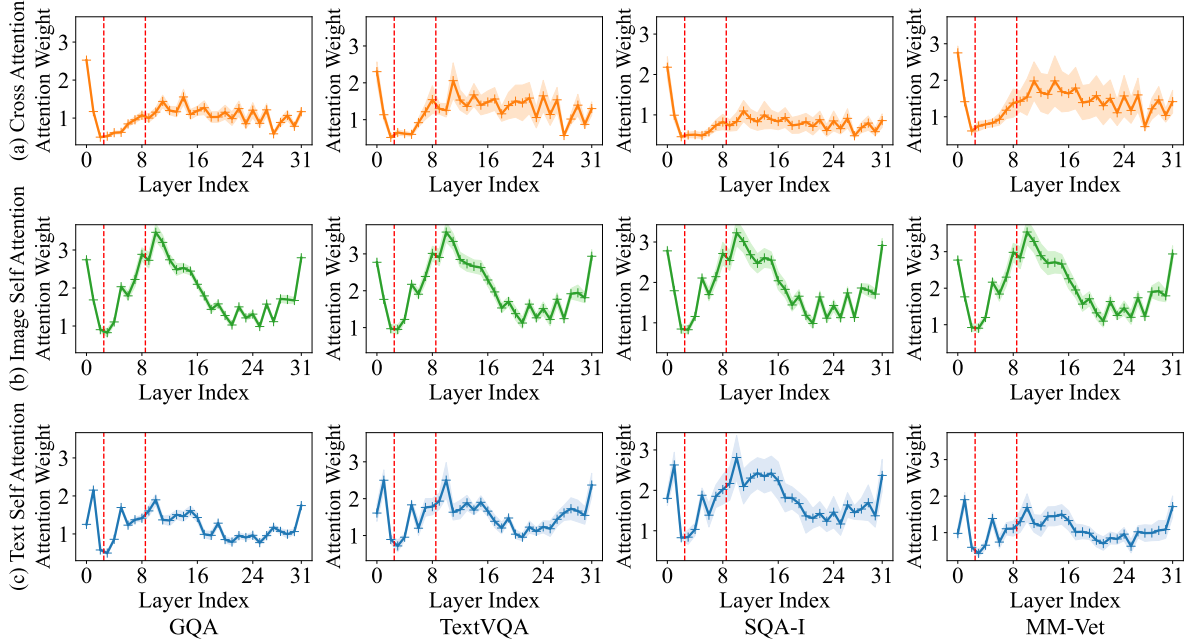


Figure 12. Distributions of averaged attention scores of image self-attention, cross-attention and text self-attention of Eagle-X5 7B. We visualize the mean and variance of the attention weight of each part on GQA, TextVQA, SQA-I, MM-Vet datasets. From these distributions, we can summarize three main stages of MLLMs as introduced in the main paper, which are then marked by red lines.

A.3. Entropy of Attention

In Fig. 13-16, we visualize the entropy distributions of cross-attention matrices and text self-attention matrices. For all these MLLMs and datasets, we can observe that removing all visual tokens at an appropriate time will not have a significant impact on the answer modeling process. Specifically, for all MLLMs and datasets, the removing of visual tokens only makes the entropy of cross-attention disappear, while the entropy of text self-attention maintains the same distribution. Overall, these results well confirm that cross-modal interaction in fact barely contributes to multimodal reasoning after some layers.

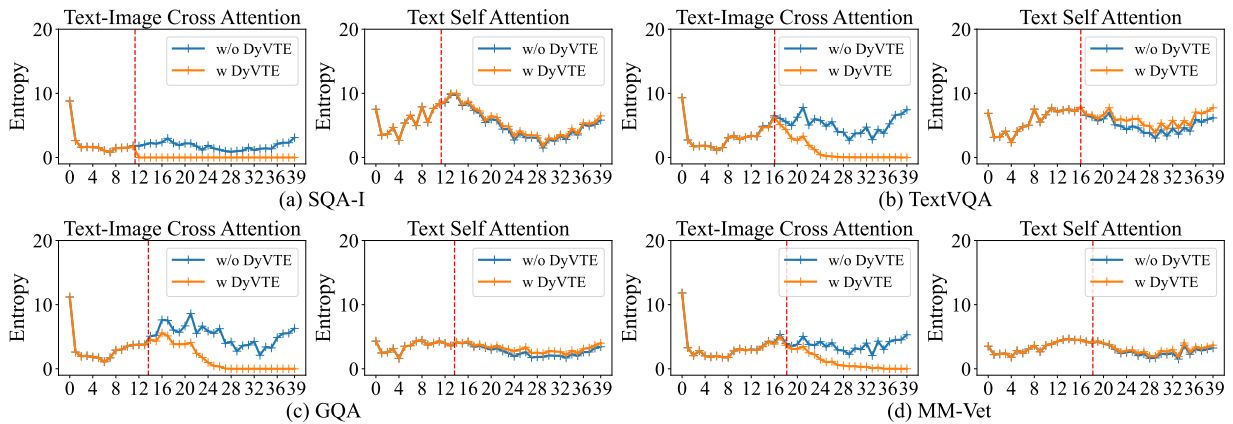


Figure 13. The entropy of two attention distributions. We visualize the entropy of cross-attention matrices and text self-attention on LLaVA-1.5 13B with and without our DyVTE, which shows that the removal of visual tokens barely affect the text self-attention.

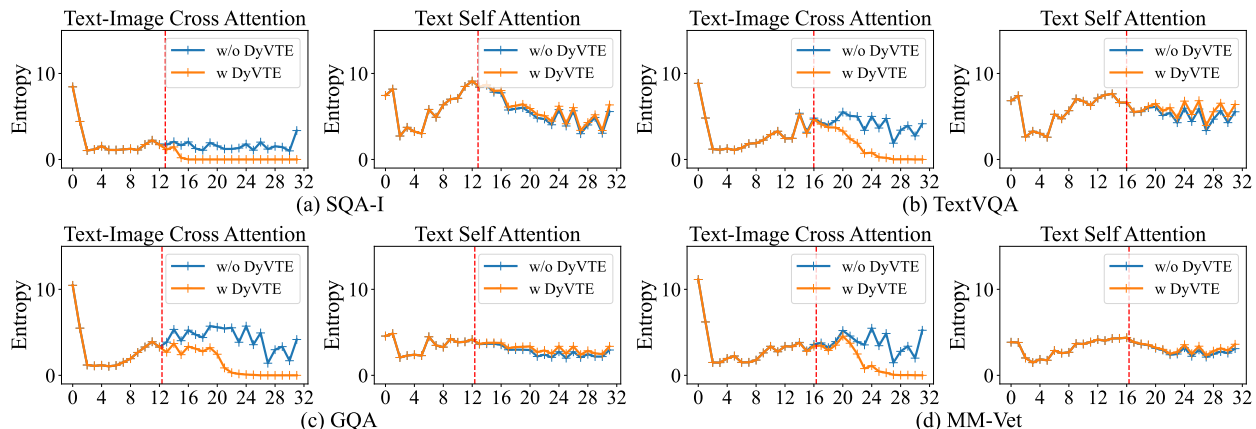


Figure 14. The entropy of two attention distributions. We visualize the entropy of cross-attention matrices and text self-attention on InternVL 7B with and without our DyVTE, which shows that the removal of visual tokens barely affect the text self-attention.

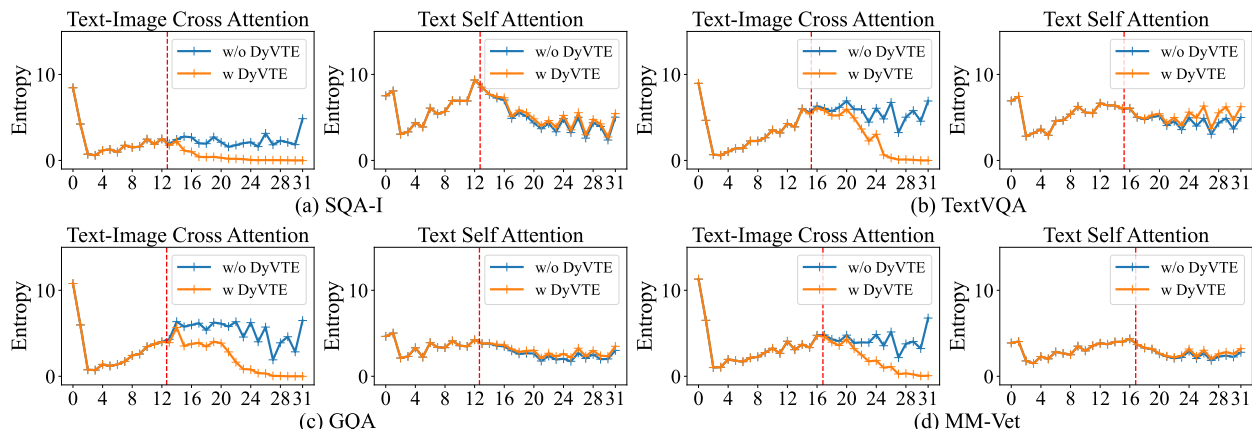


Figure 15. The entropy of two attention distributions. We visualize the entropy of cross-attention matrices and text self-attention on VILA 7B with and without our DyVTE, which shows that the removal of visual tokens barely affect the text self-attention.

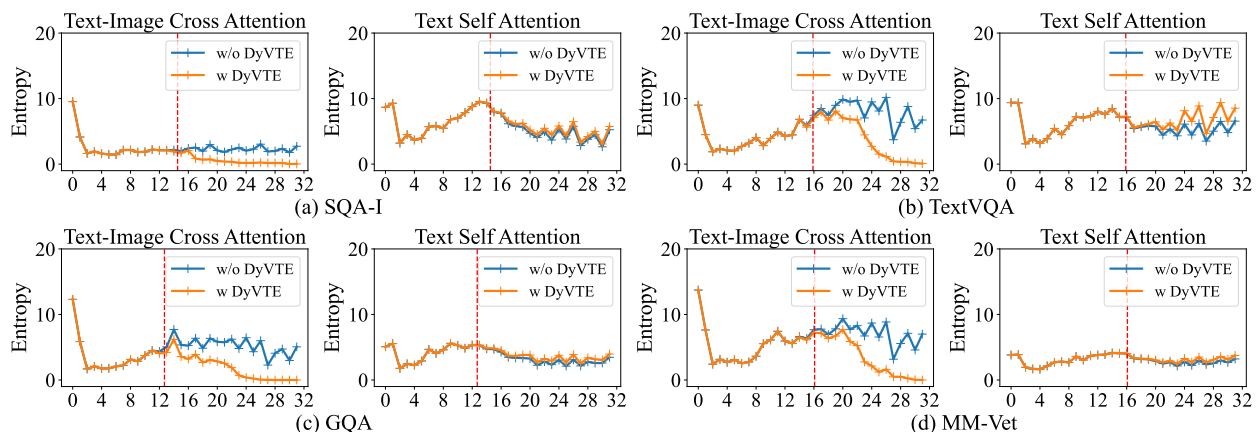


Figure 16. The entropy of two attention distributions. We visualize the entropy of cross-attention matrices and text self-attention on Eagle-X5 7B with and without our DyVTE, which shows that the removal of visual tokens barely affect the text self-attention.